Journal of Low Temperature Physics, Vol. 12, Nos. 1/2, 1973

Splitting of the Phonon Spectrum in ^{3}He–^{4}He Solutions*

David L. Bartley†

Department of Physics, University of Michigan, Ann Arbor, Michigan

John E. Robinson

Argonne National Laboratory, Argonne, Illinois

and Victor K. Wong‡

Department of Physics, University of Michigan, Ann Arbor, Michigan

(Received January 16, 1973)

The dynamic structure function for ^{4}He–^{4}He density correlations $S^{44}(\mathbf{k}, \omega)$ is calculated as a function of the wave vector **k** *and frequency ω for a simple model of a ^{3}He–^{4}He solution at various temperatures and small ^{3}He molar concentration* x. *The inputs to the model include the measured ^{4}He phonon spectrum and the zero-concentration ^{3}He quasiparticle energy (above the* $k = 0$ *value), which is taken to be quadratic in* k *and to intersect the phonon spectrum at k_c near the roton minimum. Taking into account the decay of a phonon into a quasiparticle–hole pair, which is effected in the model by a quantum hydrodynamic interaction, we find that the phonon spectrum is split into two distinct branches. At k_c the splitting of the phonon branches depends on a coupling constant γ and the crossover parameter $\varepsilon(k_c)/k_c$. If in ^{3}He–^{4}He solutions γ is large enough and $\varepsilon(k_c)/k_c$ is small enough, then the phonon spectrum is split into two branches.*

1. INTRODUCTION

Although the excitation spectrum in liquid ^{4}He has been determined directly by inelastic neutron scattering,[1] the excitation spectra of ^{3}He and

*Work performed in part under the auspices of the U.S. Atomic Energy Commission.

†Resident Student Associate, Summer 1972, at Argonne National Laboratory, Argonne, Illinois.

‡Supported in part by a Faculty Research Grant and Fellowship from the Horace H. Rackham School of Graduate Studies at the University of Michigan.

^{3}He–^{4}He systems have not been investigated in the same way, as the ^{3}He nucleus has an extremely large cross section for neutron capture. Recent developments in techniques, however, have changed the situation to the extent that neutron scattering on ^{3}He–^{4}He solutions is being considered at Argonne National Laboratory and perhaps elsewhere. In anticipation of such experiments, we have performed a simple calculation of the excitation spectrum and the ^{4}He–^{4}He dynamic structure function $S^{44}(\mathbf{k}, \omega)$ as a function of wave vector $\mathbf{k}$ and frequency ω in a model ^{3}He–^{4}He system at various temperatures T and small ^{3}He molar concentration x.

Due to the nature of inelastic neutron scattering, the region probed is confined to the collisionless regime, rather than the collision-dominated hydrodynamic regime. We take as inputs to our model the ^{4}He phonon spectrum, as measured by neutron scattering,[1] and the $x = 0$ ^{3}He quasiparticle energy (above the $k = 0$ value), which is taken to be quadratic in the wave vector $\mathbf{k}$ even for $k \gtrsim 1$ Å^{-1} and to intersect the phonon spectrum at $k_c = 1.7$ Å^{-1} and energy, $\varepsilon(k_c) = 10$ K, near the roton minimum. In the absence of a microscopic theory of the effective interaction between excitations in the short-wavelength ($k \gtrsim 1$ Å^{-1}) collisionless regime, we revert back to the phenomenological quantum-hydrodynamic theory of the effective interaction.[2–4] Although such an extrapolation of a quantum-hydrodynamic theory into the short-wavelength regime is not justified, we feel that the basic phonon–quasiparticle process included in the model calculation does shed some light on the qualitative features of the elementary excitations in ^{3}He–^{4}He solutions. The basic nontrivial process considered is the decay of a ^{4}He phonon into a ^{3}He quasiparticle–hole pair, which is incorporated into the calculation by means of the usual perturbative techniques. This process is important in that it allows phonons to make a transition into the quasiparticle–hole continuum and thus produces a splitting of the phonon spectrum into two branches.

In Section 2 the qualitative features of the density response of a coupled system are discussed. The model and a summary of the results of the model calculation are presented in Section 3, which is followed in Section 4 by a sketch of the method and approximation used in the model calculation. A brief discussion of the calculation is found in the final section.

2. QUALITATIVE FEATURES

In a ^{3}He–^{4}He system, we can define the dynamic structure function for ^{4}He–^{4}He density correlations as

$$S^{44}(\mathbf{k}, \omega) = (1/N_4) \sum_n |\langle n|\rho_{\mathbf{k}}^+|0\rangle|^2 \delta(\omega - \omega_{n0}) \tag{1}$$

where N_4 is the number of ^{4}He atoms, $\hbar\omega_{n0}$ is the excitation energy of the exact energy eigenstate $|n\rangle$ above the ground state $|0\rangle$, and $\rho_{\mathbf{k}}^+$ is the ^{4}He

density fluctuation operator. The other dynamic structure functions $S^{34}(\mathbf{k}, \omega)$ and $S^{33}(\mathbf{k}, \omega)$ can be given by relations analogous to (1) with $\rho_{\mathbf{k}}^{+}$ suitably defined.[5] If we include the phonon–quasiparticle coupling in the ^{3}He–^{4}He system, then there can be transitions between ^{4}He states and ^{3}He states. Thus any energy eigenstate $|n\rangle$ is in general a superposition of ^{4}He states and ^{3}He states, i.e., the nucleon mass number is no longer a good quantum number. Since a ^{3}He–^{4}He system is translationally invariant, the energy eigenstates $|n\rangle$ of the system can be classified in accordance to the momentum $\hbar\mathbf{k}$. Therefore, from (1) we see that the various dynamic structure functions $S^{44}(\mathbf{k}, \omega)$, $S^{34}(\mathbf{k}, \omega)$, and $S^{33}(\mathbf{k}, \omega)$ all have the same set of singularities as a function of ω for a fixed k. If $S^{44}(\mathbf{k}, \omega)$ has a δ function at $\omega(k)$, then so would $S^{34}(\mathbf{k}, \omega)$ and $S^{33}(\mathbf{k}, \omega)$, but with in general different relative strengths. In other words, the dispersion relation of a well-defined excitation is uniquely determined by the sharp peaks found in any of the dynamic structure functions, as the sharp peaks are common to all.

Keeping in mind this general feature of the sharing of singularities in the density response of a coupled system, we can illustrate the primary physical features of the present calculation with a simple model, which we shall call the neutral jellium model. Consider a system of fermions interacting with each other by a direct two-body short-ranged repulsion $V(k)$ and linearly coupled to a phonon field via density fluctuations. [This linear coupling is like the first piece of our H_{int} in Eq. (4).] In the random phase approximation (RPA), the equations of motion for density fluctuations yield a dispersion relation

$$1 = \Pi^0(\mathbf{k}, \omega)\left[V(k) + \frac{k^2}{\omega^2 - \omega_0^2(k)}|\gamma(k)|^2 \right] \tag{2}$$

where $\gamma(k)$ is the coupling function, $\omega_0(k)$ is the bare phonon frequency, and $\Pi^0(\mathbf{k}, \omega)$ is the RPA polarization propagator. If the coupling $\gamma(k)$ is zero, then, since $\Pi^0(\mathbf{k}, \omega)$ is positive above the fermion particle–hole continuum and negative below, a collective mode involving the fermions could exist only *above* the continuum. On the other hand, for nonzero coupling the phonon exchange can make the total effective interaction attractive and (coupled) collective modes can exist *below* the continuum. It is also clear from (2) that a coupled mode above (below) the continuum must also lie above (below) $\omega_0(k)$. A familiar example of a coupled mode below the continuum is found in the usual (charged) jellium model,[6] namely, the acoustic mode in which the electrons follow the ions. Here the acoustic mode remains well defined right through the continuum because the small mass ratio $(m_{\text{el}}/M_{\text{ion}})$ suppresses the decay of the mode into electron–hole pairs. In contrast, ^{3}He–^{4}He solutions with a mass ratio of the order unity can have no such stable branch penetrating the continuum.

If we let ρ_3 be the fermion density and ρ_4 be the phonon density in the neutral jellium, the linearized equations of motion give

$$\rho_4(\mathbf{k}, \omega) \propto k^2[\omega^2 - \omega_0^2(k)]^{-1}\gamma(k)\rho_3(\mathbf{k}, \omega) \tag{3}$$

From (3), we can see that the composition of the coupled modes is mainly ρ_4 for ω close to $\omega_0(k)$ and is strongly mixed for ω close to the particle–hole continuum. As the relative fermion concentration is decreased, the interesting region where the modes are strongly mixed closes in on the crossover at k_c, since Π^0 in Eq. (2) is proportional to the bare fermion density of states. If the simplest BBP[2] interaction is used in (2), there is no static instability, i.e., the lower coupled mode splits off from the continuum at finite frequency. All these qualitative features are present in the following calculation of a model ^{3}He–^{4}He system.

3. THE MODEL AND SUMMARY OF RESULTS

The model ^{3}He–^{4}He system that we consider here has three parts. First there are ^{4}He phonons with no background but with the measured ^{4}He spectrum $\omega_0(k)$ at the reduced solution density. The density dependence of $\omega_0(k)$ is estimated from the data of Henshaw and Woods.[7] Second there are ^{3}He quasiparticles with energy spectrum

$$\varepsilon_k = -|\varepsilon_0| + \hbar^2k^2/2m$$

where $m = 2.34m_3$ is the effective mass, and m_3 is the ^{3}He atomic mass. Third, there is a phonon–quasiparticle coupling, which is taken to be given by the quantum-hydrodynamic expression[4]

$$H_{\text{int}} = \int d^3x[\gamma_\rho\rho_4\rho_3 + \gamma_J\mathbf{j}_4 \cdot \mathbf{j}_3 + \tfrac{1}{2}g_\rho\rho_4^2\rho_3 + \tfrac{1}{2}g_J\mathbf{j}_4 \cdot \mathbf{j}_4\rho_3] \tag{4}$$

where the coupling constants are given by

$$\begin{aligned}
\gamma_\rho &= \partial\varepsilon_0/\partial n_4 = (1 + \alpha)m_4c_0^2/n_4 \\
\gamma_J &= \delta m/n_4 \\
g_\rho &= \partial^2\varepsilon_0/\partial n_4^2 = (m_4c_0^2/n_4)(\partial\alpha/\partial n_4) + 2(1 + \alpha)(m_4c_0/n_4)(\partial c_0/\partial n_4) \\
&\quad -(1 + \alpha)(m_4c_0^2/n_4^2) \\
g_J &= -(m_3\delta m/mn_4^2)
\end{aligned} \tag{5}$$

Here m_4 is the ^{4}He atomic mass, $\delta m = m - m_3$, c_0 is the ^{4}He sound speed, $1 + \alpha = 1.28$ is the average number of ^{4}He atoms displaced by a ^{3}He

atom, and n_4 is the density of pure ^{4}He. The ^{4}He phonon density and current operators in the interaction picture are

$$\begin{aligned}\rho_4(\mathbf{x}, t) &= \sum_k [\hbar k^2 n_4/2m_4\omega_0(k)\Omega]^{1/2}\{b_{\mathbf{k}}\, e^{i[\mathbf{k}\cdot\mathbf{x}-\omega_0(k)t]} + b_{\mathbf{k}}^+\, e^{-i[\mathbf{k}\cdot\mathbf{x}-\omega_0(k)t]}\} \\ \mathbf{j}_4(\mathbf{x}, t) &= \sum_k [\hbar\omega_0(k) n_4/2m_4\Omega]^{1/2}\hat{\mathbf{k}}\{b_{\mathbf{k}}\, e^{i[\mathbf{k}\cdot\mathbf{x}-\omega_0(k)t]} + b_{\mathbf{k}}^+\, e^{-i[\mathbf{k}\cdot\mathbf{x}-\omega_0(k)t]}\}\end{aligned} \tag{6}$$

where $b_{\mathbf{k}}$ and $b_{\mathbf{k}}^+$ are the phonon annihilation and creation operators, and Ω is the volume. The ^{3}He quasiparticle density and current operators are

$$\begin{aligned}\rho_3(\mathbf{x}, t) &= \psi^+(\mathbf{x}, t)\psi(\mathbf{x}, t) \\ \mathbf{j}_3(\mathbf{x}, t) &= (\hbar/2mi)\{\psi^+(\mathbf{x}, t)\nabla\psi(\mathbf{x}, t) - [\nabla\psi^+(\mathbf{x}, t)]\psi(\mathbf{x}, t)\} \\ \psi(\mathbf{x}, t) &= \Omega^{-1/2}\sum_k a_{\mathbf{k}}\, e^{i[\mathbf{k}\cdot\mathbf{x}-(\varepsilon_k t/\hbar)]}\end{aligned} \tag{7}$$

where $a_{\mathbf{k}}$ is the quasiparticle annihilation operator.

The quantity of interest in a neutron scattering experiment is the dynamic structure function. Since $S^{44}(\mathbf{k}, \omega)$ dominates the dynamic structure function for the ^{3}He–^{4}He system with small ^{3}He molar concentration x, we focus our attention on the calculation of $S^{44}(\mathbf{k}, \omega)$. Thus whenever there exists no ambiguity, we shall call (1) simply the dynamic structure function and suppress the superscript 44.

We now summarize the results of our model calculation, performed by using the simple perturbative approximation which is discussed in the next section. The dynamic structure function $S(\mathbf{k}, \omega)$ is found to have three distinct modes at $T = 0$: two "phonon" branches given by

$$S_\pm(\mathbf{k}, \omega) = S_\pm(k)\delta[\omega - \omega_\pm(k)]$$

which correspond to the phonon splitting discussed in Sections 1 and 2, and an incoherent "particle–hole" mode $S_{\text{inc}}(\mathbf{k}, \omega)$, which represents the excitation of a virtual "phonon" that decays into a real "quasiparticle–hole" pair. All these modes are, of course, coupled modes, and the identification of each mode with a particular ^{3}He or ^{4}He mode is made in the spirit of perturbation theory. Figures 1 and 2 display the two "phonon" branches $\omega_\pm(k)$, for $x = 0.001$ and 0.01, respectively. At k_c and $\varepsilon(k_c)$, where the $x = 0$ ^{3}He quasiparticle spectrum crosses the ^{4}He phonon spectrum, the energies of the two "phonon" branches are given by

$$\hbar\,\mathrm{Re}\,\omega_\pm(k_c, x) = \varepsilon(k_c) \pm \gamma\sqrt{x} \tag{8a}$$

provided

$$k_F\varepsilon(k_c)/k_c \ll \gamma\sqrt{x} \ll \varepsilon(k_c) \tag{8b}$$

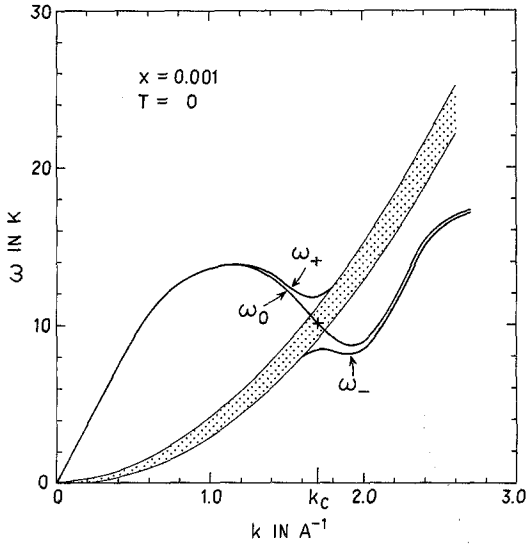

Fig. 1. The "phonon" spectrum at $x = 0.001$ and $T = 0$. ω_0 is the ^{4}He phonon spectrum, the cross-hatched region represents the ^{3}He quasiparticle–hole continuum for $x = 0.001$, and $\omega_\pm$ is the split phonon spectrum calculated for $x = 0.001$. The cross denotes the crossing of ω_0 with the ^{3}He quasiparticle spectrum.

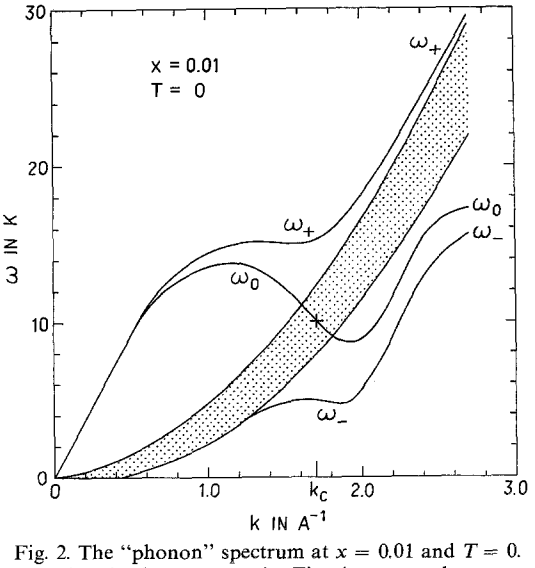

Fig. 2. The "phonon" spectrum at $x = 0.01$ and $T = 0$. Notation is the same as in Fig. 1, except that now $x = 0.01$.

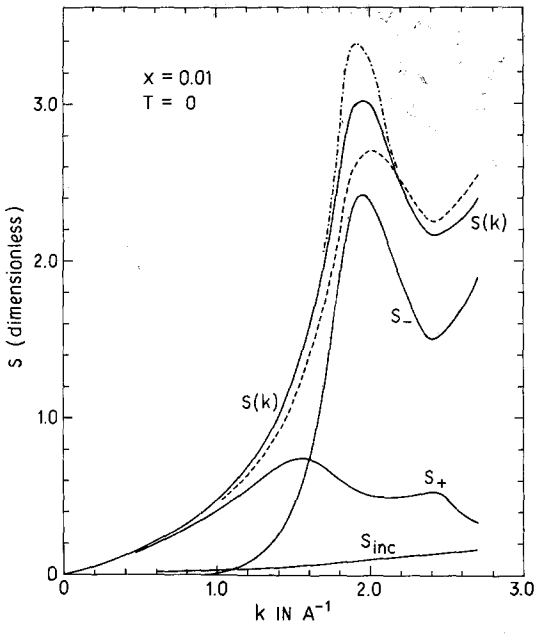

Fig. 3. Static structure function $S(k)$ at $x = 0.01$ and $T = 0$. $S_\pm$ corresponds to the $\omega_\pm$ "phonon" mode, $S_{\rm inc}$ corresponds to the "quasiparticle–hole" mode, and $S(k) = S_+ + S_- + S_{\rm inc}$. To display the dependence of $S(k)$ in x and T, the static structure function at $x = 0$ and $T = 0$ (dash line) and the static structure function at $x = 0.01$ and $T = 1.25$ K (dash–dot line) are also plotted.

where k_F is the Fermi wave vector, $\varepsilon(k_c) = \hbar^2 k_c^2/2m$, and

$$\gamma = c_0^2\sqrt{mm_4}\{1 + \alpha + (\delta m/m_4)[\varepsilon(k_c)/2mc_0^2]\} \approx 50\,\text{K} \tag{8c}$$

The static structure functions for the three modes $S_\pm(k)$ and $S_{\rm inc}(k) = \int_0^\infty d\omega S_{\rm inc}(k, \omega)$ are plotted in Fig. 3. Note that $S_+(k)$ dominates for small $k < 1.6$ Å^{-1}, $S_-(k)$ dominates for large $k > 1.6$ Å^{-1}, and $S_{\rm inc}(k)$ is a small correction over the entire range of k considered.

The two sharp "phonon" branches at $T = 0$ are broadened considerably at finite temperatures, as can be seen in Fig. 4, where $S(\mathbf{k}, \omega)$ at $x = 0.01$ and $k = 1.6$ Å^{-1} is plotted as a function of ω for two temperatures $T = 0.1$ and 1.25 K. Explicitly, the width of the two "phonon" branches is given by

$$\hbar\,\text{Im}\,\omega_\pm(k_c, x) = -(\sqrt{\pi}/4)\gamma^2 x\sqrt{\beta/\varepsilon(k_c)}\exp[-\gamma^2\beta x/4\varepsilon(k_c)] \tag{9a}$$

provided

$$k_B T_F \ll \beta^{-1} = k_B T \ll \varepsilon(k_c) \tag{9b}$$

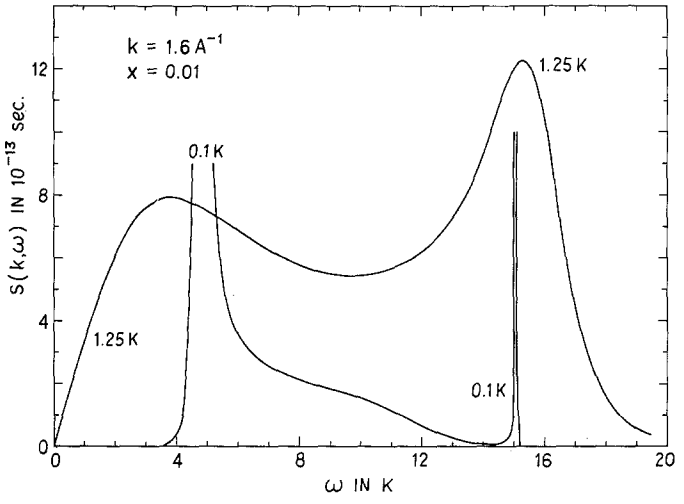

Fig. 4. Dynamic structure function $S(k, \omega)$ as a function of ω with $k = 1.6$ Å^{-1} and $x = 0.01$ for two temperatures, $T = 0.1$ and 1.25 K.

where T_F is the Fermi temperature. In Fig. 5, $S(\mathbf{k}, \omega)$ at $x = 0.01$ and $T = 1.25$ K is plotted as a function of ω for various wave vectors near k_c. Note the fairly sharp transition from the (+) to the (−) phonon branch as k is increased through k_c.

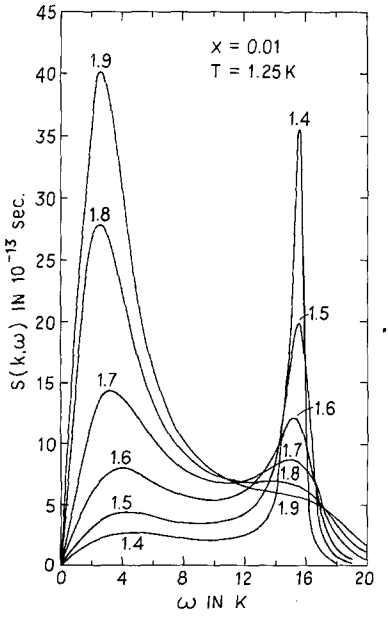

Fig. 5. Dynamic structure function $S(k, \omega)$ as a function of ω with $x = 0.01$ and $T = 1.25$ K for various wave vectors k near the crossing $k_c = 1.7$ Å^{-1}. The labels attached to each curve are the values of k per angstrom.

From the above results of the model calculation, it appears almost certain that in ^{3}He–^{4}He solutions the ^{4}He phonon spectrum would be split in some manner by the ^{3}He quasiparticle–hole continuum. An obvious exception would arise if the $x = 0$ ^{3}He quasiparticle spectrum (above the $k = 0$ value) does not cross the phonon spectrum. A rigid shift of the ^{3}He quasiparticle spectrum, i.e., of the $k = 0$ value, has no consequence since it does not change the particle–hole continuum at all. Instead, the quasiparticle spectrum would have to be sufficiently distorted that the entire intersection of the continuum with the phonon spectrum $\omega_0(k)$ were eliminated. Barring this exception, we conjecture that some splitting is bound to occur as long as the transition from phonon to quasiparticle–hole pair is not forbidden. Thus the fact that the quantum–hydrodynamic effective interaction, rather than a microscopic short-wavelength effective interaction, was used in the model calculation does not affect the existence of some splitting of the phonon spectrum, although it probably overestimates the magnitude.

4. THE CALCULATION

The $T = 0$ calculation proceeds by means of straightforward diagrammatic perturbation techniques.[8] Each of the four terms in the above [Eq. (4)] interaction Hamiltonian H_{int} may be represented by a vertex, as shown in Fig. 6—the solid circles representing ^{4}He phonon density vertices and the open circles denoting ^{4}He phonon current vertices. Any diagram may be constructed by joining these vertices by solid and wiggly lines representing quasiparticle and phonon propagators, respectively.

We center our attention on the phonon density–density propagator $D_{11}(k, \omega)$, defined as the four-dimensional Fourier transform of $D_{11}(\mathbf{x}t, \mathbf{x}'t')$, which at zero temperature is given by

$$D_{11}(\mathbf{x}t, \mathbf{x}'t') = -i\langle\psi_0|T[\rho(\mathbf{x}, t)\rho(\mathbf{x}', t')]|\psi_0\rangle \tag{10}$$

where T is the time-ordering operator, $\rho(\mathbf{x}, t)$ is the phonon density (6) in the Heisenberg picture, and $|\psi_0\rangle$ is the exact normalized ground state. The dynamic structure function, Eq. (1), is given by

$$S(\mathbf{k}, \omega) = -(1/\pi n_4)\,\text{Im}\, D_{11}^R(\mathbf{k}, \omega) \tag{11}$$

where D_{11}^R is the retarded density–density propagator. Because of the various terms present in the interaction (4), it is convenient to introduce the phonon

Fig. 6. The four vertices corresponding to the four terms in H_{int}, Eq. (4). Solid circles represent ^{4}He phonon density vertices, and open circles denote ^{4}He phonon current vertices.

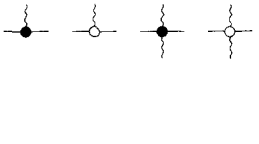

density–current propagator $D_{12}(\mathbf{k},\omega)$ and the current–current propagator $D_{22}(\mathbf{k},\omega)$. These four propagators can be conveniently grouped into a 2×2 symmetric matrix D_{ij} which satisfies a matrix Dyson equation

$$D_{ij} = D_{ij}^0 + D_{ik}^0 \Sigma_{kl} D_{lj} \tag{12}$$

where Σ_{ij} is the matrix self-energy and D_{ij}^0 is the ^{4}He phonon propagator, i.e., the propagator D_{ij} in the limit $x \to 0$ or when the interaction (4) is turned off. Note that the propagator D_{ij}^0 is taken to have the form of a bare phonon propagator with no background [see Eq. (13c) below]. Hence in the limit $x \to 0$, the static structure function $S(k)$ (see Fig. 3) is given by the Feynman relation

$$S(k) = \hbar k^2 / 2m\omega_0(k)$$

which overestimates the value of $S(k)$ near the roton minimum.

The calculation proceeds in the usual fashion by approximating Σ_{ij}, which we take to be the diagrams shown in Fig. 7. Equation (12) can then be solved, yielding for the retarded density–density propagator

$$D_{11}^R = A/(D_0^{-1} - \Sigma^R) \tag{13a}$$

$$A = 1 + (\gamma_J^2 \omega^2 n_4 / m_4 k^2)\Pi^{0R} - [(\gamma_J^2 m^{-1} - g_J) n_4^2 x / m_4] \tag{13b}$$

$$D_0 = D_{11}^0 = (\hbar k^2 n_4 / m_4)(\omega^2 - \omega_0^2)^{-1} \tag{13c}$$

$$\begin{aligned} \hbar\Sigma^R = {} & [\gamma_\rho^2 + 2\omega^2 k^{-2} \gamma_\rho \gamma_J + \omega_0^2 \omega^2 k^{-4} \gamma_J^2]\Pi^{0R} \\ & + [g_\rho - (\gamma_J^2 m^{-1} - g_J)\omega_0^2 k^{-2}] n_4 x \end{aligned} \tag{13d}$$

$$\Pi^{0R} = [\mathrm{Re} + i\,\mathrm{sgn}\,(\omega)\,\mathrm{Im}]\Pi^0 \tag{13e}$$

and where $\Pi^0(\mathbf{k}, \omega)$ has been evaluated[9] in terms of elementary functions

$$\begin{aligned} \mathrm{Re}\,\Pi^{0R}(\mathbf{k},\omega) = {} & \frac{2mk_F}{4\pi^2\hbar^2} \left\{ -1 + \frac{1}{2q}\left[1 - \left(\frac{v}{q} - \frac{q}{2}\right)^2\right] \ln\left|\frac{1 + [(v/q) - (q/2)]}{1 - [(v/q) - (q/2)]}\right| \right. \\ & \left. - \frac{1}{2q}\left[1 - \left(\frac{v}{q} + \frac{q}{2}\right)^2\right] \ln\left|\frac{1 + [(v/q) + (q/2)]}{1 - [(v/q) + (q/2)]}\right| \right\}, \end{aligned} \tag{14}$$

where $v = \omega m/\hbar k_F^2$ and $q = k/k_F$.

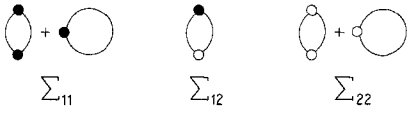

Fig. 7. The approximation to the self-energy matrix used in the model calculation. The solid lines represent quasiparticle propagators, and the vertices are as in Fig. 6.

We now obtain the mode splitting at k_c. We seek the solution $\omega = \omega(k_c)$ of $D_0^{-1} - \Sigma^R = 0$. Letting $\delta\omega = \omega(k_c) - \hbar k_c^2/2m = \omega(k_c) - \omega_0(k_c)$, we have from (13)

$$(\hbar k_c^2 n_4/m_4) D_0^{-1} = \omega(k_c)^2 - \omega_0(k_c)^2$$
$$= (\hbar k_c^2/m)\delta\omega + O[(\delta\omega)^2] \tag{15}$$

assuming that $\delta\omega \ll \hbar k_c^2/m$. As we shall see from (17)–(19) that at k_c Re $\Pi^{0R} = O(x^{1/2})$, we have from (13)

$$\hbar\Sigma^R = \{\gamma_\rho + [\varepsilon(k_c)/2m]\gamma_J\}^2 \text{ Re } \Pi^{0R} + O(x) \tag{16}$$

It is easily shown in the regime $q^2 \gg \delta v = (v - q^2)/2 \gg q$ that (14) reduces to

$$\text{Re } \Pi^{0R} \approx (mk_F/\hbar^2 3\pi^2 \delta v) \tag{17}$$

Since $\delta v = \delta\omega m/\hbar k_F^2$ at k_c, we have from (15)–(17)

$$D_0^{-1} - \Sigma^R = (m_4/mn_4)\delta\omega - (k_F^3/3\pi^2\hbar^2)(1/\delta\omega)[\gamma_\rho + (1/2m)\varepsilon(k_c)\gamma_J]^2 \tag{18}$$

Setting (18) equal to zero and $k_F^3/3\pi^2 n_4 = x$, we find the square of the splitting

$$(\hbar\delta\omega)^2 = (n_4^2 m/m_4)[\gamma_\rho + (1/2m)\varepsilon(k_c)\gamma_J]^2 x \tag{19}$$

The above expression may be written in the form $\hbar\delta\omega = \pm\gamma\sqrt{x}$, thus yielding (8) with the regime of validity (8b) arising from the restriction on (17).

The analogous $T > 0$ calculation is reasonably easily accomplished for the regime of interest $T \gg T_F$ under the assumption that the fermions obey Boltzmann statistics. The only resulting change in the above equations is the expression for the retarded Π^{0R}, which has been expressed[10] in a form amenable to calculation. Equation (9) then easily follows.

The other results for $k \neq k_c$, which have been summarized in Figs. 1–5 in Section 3, were obtained by numerical methods. In addition, we have verified that the f-sum rule is satisfied to $O(x)$.

We finally make a brief calculation of the sound speed shift to $O(x)$ at $T = 0$ to make contact with Ref. 3. The sound speed is ascertained by finding the poles of D^R for small k; i.e., we wish to solve

$$\{D_0[\mathbf{k}, \omega(k)]\}^{-1} = \Sigma^R[\mathbf{k}, \omega(k)] \tag{20}$$

in the limit $k \to 0$. The pure ^{4}He phonon spectrum $\omega_0(k)$ at the reduced solution density, $n_4 + \delta n_4 = n_4[1 - (1 + \alpha)x]$, is given by

$$\omega_0(k) = c_0 k[1 + (\delta n_4/c_0)(\partial c_0/\partial n_4] + \cdots$$
$$= c_0 k[1 - (1 + \alpha)(x n_4/c_0)(\partial c_0/\partial n_4] + \cdots \tag{21}$$

With $\omega(k) \to c(x)k$ as $k \to 0$, we have from (13)

$$\{D_0[\mathbf{k}, \omega(k)]\}^{-1} = (2m_4c_0/\hbar n_4)\{c(x) - c_0[1 - (1 + \alpha)(xn_4/c_0)(\partial c_0/\partial n_4)]\} \quad (22)$$

Thus, from (20) and (22)

$$c(x) = c_0[1 - (1 + \alpha)(xn_4/c_0)(\partial c_0/\partial n_4)] + (\hbar n_4/2m_4c_0) \lim_{k\to 0} \Sigma^R(\mathbf{k}, kc_0) \quad (23)$$

As it is possible to show[9] that

$$\lim_{k\to 0} [\Pi^{0R}(\mathbf{k}, kc_0)] = xn_4/mc_0^2 \quad (24)$$

to first order in x, the expression (13) for Σ^R yields

$$\begin{aligned} \lim_{k\to 0} \hbar\Sigma^R(\mathbf{k}, kc_0) = x(m_4c_0^2/n_4)\{&(m_4/m)[1 + \alpha + (\delta m/m_4)]^2 \\ &+ (1 + \alpha)[(2n_4/c_0)(\partial c_0/\partial n_4) - 1] \\ &+ n_4(\partial\alpha/\partial n_4) - (\delta m/m_4)\} \end{aligned} \quad (25)$$

Substituting (25) into (23), we obtain to first order in x

$$\begin{aligned} c(x) = c_0 + \tfrac{1}{2}c_0x\{&(m_4/m)[1 + \alpha + (\delta m/m_4)]^2 - (1 + \alpha) \\ &+ n_4(\partial\alpha/\partial n_4) - (\delta m/m_4)\} \end{aligned} \quad (26)$$

which agrees with Ref. 3.

5. CONCLUDING REMARKS

We have calculated the dynamical structure function[5]

$$S(\mathbf{k}, \omega) = (1 - x)S^{44}(\mathbf{k}, \omega) + 2\sqrt{x}\sqrt{1 - x}\,S^{34}(\mathbf{k}, \omega) + xS^{33}(\mathbf{k}, \omega) \quad (27)$$

for small x at $T \geq 0$ for which limit $S(\mathbf{k}, \omega) \approx S^{44}(\mathbf{k}, \omega)$. To extend the theory to accommodate larger and physically attainable concentrations, the last two terms in (27) must be taken into account, yielding corrections of the order of $\sqrt{x}$ for $k \approx k_c$ and x for $k \approx 0$ to primarily the strengths of the coherence singularities of $S(\mathbf{k}, \omega)$. Corrections of the same order of magnitude to the positions in $(\mathbf{k}, \omega)$ space and strengths of these singularities arise from higher order contributions to S^{44} and furthermore from the direct interaction between ^{3}He quasiparticles, which has been ignored. Another process ignored is the three-phonon process, which will give rise to a background in $S(\mathbf{k}, \omega)$ as well as to a lowering of the values of $S(k)$ near the roton minimum. It is clear that additional analysis is required for interpretation of experiments at higher concentrations than we have considered, and such analysis is underway.

Light scattering depends only on $S(\mathbf{k}, \omega)$, whereas in the neutron cross section the dynamic structure functions $S^{\alpha\beta}(\mathbf{k}, \omega)$ are weighted by different combinations of the nuclear scattering lengths a_3 and a_4. However, since $S^{\alpha\beta}(\mathbf{k}, \omega)$ have the same set of singularities, neutron scattering would be able to pick out $\omega_{\pm}(k)$. Lastly, it seems clear that for the ^{3}He–^{4}He system the second-order Raman spectra, as well as the neutron spectra, may show striking changes from that of pure ^{4}He.

The splitting of the phonon spectrum into two branches can be discussed in terms of the representative splitting at the crossover k_c. In our model system at $T = 0$, the splitting at k_c as given by (8a) is valid only if the inequality (8b) is satisfied. This inequality requires the splitting at k_c to be much smaller than the crossover energy $\varepsilon(k_c) \approx 10$ K but much larger than the half-width of the quasiparticle–hole continuum, i.e., $2\varepsilon(k_c)k_F/k_c \approx 2(9\text{ K})x^{1/3}$. In other words, if the inequality (8b) is satisfied, then the splitting at k_c would result in two distinct branches outside the quasiparticle–hole continuum. As $x \to 0$ with all other parameters fixed, it is clear that the inequality (8b) would not be satisfied and that the spectrum would not remain outside the continuum. Therefore for a fixed concentration x, there exist two physical parameters, the effective coupling constant γ and the crossover parameter $\varepsilon(k_c)/k_c$, that determine in large measure the visibility of the splitting of the phonon spectrum into two branches in ^{3}He–^{4}He solutions at $T = 0$.

It is not known whether the $x = 0$ ^{3}He quasiparticle spectrum intersects the ^{4}He phonon spectrum. To perform our model calculation, we have assumed for all k a quasiparticle spectrum proportional to k^2. The leading small-k correction to the k^2 quasiparticle spectrum is usually expressed in terms of a k^4 term with a negative coefficient. The effect of such a correction if extrapolated beyond its range of validity is to lower the crossover parameter $\varepsilon(k_c)/k_c$ and hence to enhance the visibility of the splitting into two branches.

The effective coupling constant γ can be interpreted as the phonon absorption amplitude at k_c. Since the estimate (8c) is based on an extrapolation of the quantum hydrodynamic parameters into the short wavelength region near k_c, it is probably an overestimate of the physical value of γ. From the inequality (8b), we see that there exists a value of γ below which the spectrum no longer remains outside the quasiparticle–hole continuum. Taking the model crossover parameters, $\varepsilon(k_c) \approx 10$ K and $k_c \approx 1.7\text{ A}^{-1}$, we find that the physical value of γ must be greater than 9 K in order that the spectrum consist of two branches outside the continuum. Hence we expect a reduction in the splitting into two branches due to a smaller physical value of γ, whereas a smaller physical value of $\varepsilon(k_c)/k_c$ leads to an enhancement of the visibility of the splitting. The determination of these physical parameters, γ and $\varepsilon(k_c)/k_c$, is obviously important and awaits further experimental data.

At finite temperatures the quasiparticle–hole continuum broadens and its boundaries become diffuse. At $T \gg T_F$ a measure of the half-width of the continuum at k_c is approximately given by[10] $2[\varepsilon(k_c)k_B T]^{1/2}$. If we use this estimate of the continuum half-width in place of the $T = 0$ half-width in (8b), we see that increasing the temperature would decrease the visibility of the splitting into two branches. If in ^{3}He–^{4}He solutions γ is large enough and $\varepsilon(k_c)/k_c$ is small enough to ensure a splitting into two branches, then the observation of such a splitting is most favorable at low temperatures.

We have considered only the case in which the phonon spectrum is split into two distinct branches outside the quasiparticle–hole continuum. Calculations and discussions of the effect of ^{3}He on the phonon spectrum within the quasiparticle–hole continuum when (8b) is not satisfied are reserved for a future publication.

ACKNOWLEDGMENTS

We wish to acknowledge a number of useful conversations with W. Massey, D. L. Price, J. M. Rowe, C.-W. Woo, and M. D. Yim.

REFERENCES

1. R. A. Cowley and A. D. B. Woods, *Can. J. Phys.* **49**, 177 (1971).
2. J. Bardeen, G. Baym, and D. Pines, *Phys. Rev. Letters* **17**, 372 (1966); *Phys. Rev.* **156**, 207 (1967).
3. G. Baym, *Phys. Rev. Letters* **18**, 71 (1967).
4. G. Baym and C. Ebner, *Phys. Rev.* **164**, 235 (1967); W. F. Saam, *Ann. Phys. (N.Y.)* **53**, 219 (1969).
5. H.-T. Tan, C.-W. Woo, and F. Y. Wu, *J. Low Temp. Phys.* **5**, 261 (1971).
6. See, for example, D. Pines, *Elementary Excitations in Solids* (W. A. Benjamin, New York, 1963), Chap. 5.
7. D. G. Henshaw and A. D. B. Woods, *Proc. 7th Int. Conf. Low Temp. Phys.*, G. Graham and A. Hollis Hallett, eds. (North-Holland, Amsterdam, 1961), p. 539.
8. A. Fetter and J. Walecka, *Quantum Theory of Many-Particle Systems* (McGraw-Hill, New York, 1971).
9. See Ref. 8, pp. 158–163.
10. See Ref. 8, pp. 303–305.